X-ray QPOs from the Ultra-luminous X-ray Source in M82: Evidence Against Beaming

Tod E. Strohmayer and Richard F. Mushotzky

Laboratory for High Energy Astrophysics,
NASA's Goddard Space Flight Center, Greenbelt, MD 20771

stroh@clarence.gsfc.nasa.gov

ABSTRACT

We report the discovery with the EPIC CCD cameras onboard XMM-Newton of a 54 mHz quasiperiodic oscillation (QPO) in the > 2 keV X-ray flux from the ultra-luminous X-ray source (ULX) X41.4+60 in the starburst galaxy M82. This is the first detection of a QPO in the X-ray flux from an extra-Galactic ULX, and confirms that the source is a compact object. The QPO is detected in the combined PN and MOS data at the $\approx 6\sigma$ level, and separately at lower significances in both the PN and MOS instruments. It had a centroid frequency of 54.3 ± 0.9 mHz, a coherence $Q \equiv \nu_0/\Delta\nu_{fwhm} \approx 5$, and an amplitude (rms) in the 2 - 10 keV band of 8.5%. Below about 0.2 Hz the power spectrum can be described by a power-law with index ≈ 1, and integrated amplitude (rms) of 13.5%. The X-ray spectrum requires a curving continuum, with a disk-blackbody (diskbb) at $T = 3.1$ keV providing an acceptable, but not unique, fit. A broad Fe line centered at 6.55 keV is required in all fits, but the equivalent width (EW) of the line is sensitive to the choice of continuum model. There is no evidence of a reflection component. The implied bolometric luminosity is $\approx 4 - 5 \times 10^{40}$ ergs s^{-1}. Data from several archival Rossi X-ray Timing Explorer (RXTE) pointings at M82 also show evidence for QPOs in the 50 - 100 mHz frequency range. Several Galactic black hole candidates (BHCs), including GRS 1915+105, GRO J1655–40, and XTE 1550–564, show QPOs in the same frequency range as the 50 - 100 mHz QPOs in X41.4+60, which at first glance suggests a possible connection with such objects. However, strong, narrow QPOs provide solid evidence for disk emission, and thus present enormous theoretical difficulties for models which rely on either geometrically or relativistically beamed emission to account for the high X-ray luminosities. We discuss the implications of our findings for models of the ULX sources.

Subject headings: black hole physics - galaxies: individual: M82 - galaxies: starburst - stars: oscillations - X-rays: stars - X-rays: galaxies

1. Introduction

Many nearby galaxies harbor highly luminous point-like X-ray sources which are not associated with the nuclear region of the galaxy. Their existence has been known for some time and was first inferred from observations with the EINSTEIN observatory (Fabbiano 1988). These ultra-luminous X-ray sources (ULXs) can have apparent isotropic X-ray luminosities of $10-1000\times$ the Eddington limit for a canonical neutron star. Although some of them may be highly luminous young supernova remnants, the presence of significant time variability on timescales of days to years argues for a compact accretor (see Ptak & Griffiths 1999; Fabbiano & Trinchieri 1987; Schlegel 1994). These findings have led to the suggestion that they may represent a new class of intermediate mass ($50-1000\ M_{\odot}$) black holes (Colbert & Mushotzky 1999; Makishima et al. 2000), perhaps formed as a result of binary interactions in dense stellar environments (see for example, Portegies Zwart & McMillan 2002).

Current models for these objects center around two alternatives; (1) They are massive (50 - 1000 $M_{\odot}$) black holes radiating at or near the Eddington limit, or (2) they are more or less "normal" (ie. stellar mass) accreting compact binaries whose energy loss appears super-Eddington because it is beamed. Each of these explanations is not without its difficulties. For example, if they are massive black holes, then standard accretion disk theory suggests that they should have lower disk temperatures than stellar mass black holes. Spectroscopy with ASCA (Makishima et al. 2000), however, does not support this conclusion unless, perhaps, they are rapidly rotating Kerr holes (see, however, a recent report by Miller et al. 2002 suggesting a cooler disk in one source). Moreover, formation scenarios for IMBHs are challenging, as is the need to feed the black hole at the requisite accretion rates. Because of some of these difficulties, King et al. (2001) have argued for an association with "standard" X-ray binaries whose emission is beamed geometrically by factors of $\sim 10-100$ (see also Zezas & Fabbiano 2002). Recently, Grimm, Gilfanov & Sunyaev (2002) have demonstrated a connection between high mass X-ray binaries (HMXBs) and star formation. This association supports the putative link between star formation and ULXs, and suggests they may represent the high mass end of the luminosity function of HMXBs. However, optical searches for the high mass counterparts of the ULXs have not so far been very productive, and details of how and indeed if sufficient beaming occurs at high mass accretion rates are not well understood theoretically (Madau 1988; Kubota, Done & Makishima 2002).

There is now an extensive amount of information on the timing properties of Galactic black holes. In particular, RXTE observations of black hole candidates have discovered QPOs with frequencies ranging from 0.001 to 450 Hz (see Remillard et al., 2002 for a brief summary). Many of these QPOs are strongly correlated with spectral states. If ULXs are extragalactic analogs of the stellar mass compact binaries in our own galaxy, then they should

show some of the same timing properties and spectral correlations. Although these objects are faint by Galactic BHC standards, as we demonstrate here, the brightest sources are good candidates for low frequency ($\sim 1 - 100$ mHz) QPO searches with large area, imaging instruments, such as the EPIC CCDs onboard XMM/Newton. This possibility has led us to examine the timing properties of some of the brighter ULXs which have been observed with XMM/Newton and Chandra.

One of the brightest ULXs is the source in M82. Based on ASCA data Ptak & Griffiths (1999) found both spectral and temporal variability in the hard X-ray flux from M82. Based on the variability and high luminosity they suggested that the hard X-ray flux is from a compact object of $\approx 500 M_{\odot}$. Recent Chandra HRC observations confirm that the ULX is not associated with the dynamical center of M82 nor is it associated with any radio AGN candidate or optically bright counterpart (Kaaret et al. 2001; Matsumoto et al. 2001). Here we report timing and spectroscopy of this object (hereafter M82 X41.4+60 or simply X41.4+60) utilizing XMM/Newton and RXTE archival data. With XMM we detect a 54 mHz QPO in the hard X-ray flux from this object. We also find indications of 50 - 100 mHz QPOs from RXTE observations. We present evidence for a broad Fe Kα emission feature in the XMM spectrum. We discuss the implications of these findings for the nature of X41.4+60 and other ULXs as well.

2. XMM Observations and Data Analysis

XMM/Newton observed M82 for 30 ksec on May 5, 2001 at 09:19:40 (UT). These data are now in the public XMM archive. For our study we used only the EPIC data. We used the standard SAS version 5.3.3 tools to filter and extract images and event tables for both the PN and MOS cameras. These instruments were in PrimeFullWindow mode with the medium blocking filter. We began by extracting images from both the PN and MOS cameras. The central region of M82 has been resolved by Chandra (see Kaaret et al. 2001; Matsumoto et al. 2001). The XMM images are dominated by a bright point source, the centroid of which is consistent with the position of the brightest source detected in the Chandra HRC images (M82 X41.4+60). At XMM's spatial resolution, the field is crowded by several fainter sources resolved by Chandra, however, the XMM images strongly indicate that the flux is dominated by X41.4+60. Previous measurements indicate that the central region of M82 has substantial diffuse, soft thermal emission. We see this diffuse component in both the EPIC images and spectra (see Figure 4). Inside an 18" extraction radius the emission from the thermal component is $< 10\%$ of the point source at $E > 2$ keV, therefore, to increase the sensitivity to variability from the compact source we use only the hard X-rays (> 2 keV)

for our timing study. To investigate the source's temporal variability we extracted events from the PN and MOS cameras within a 18" circular region around the bright point source. To make the most sensitive search we combined data from the PN and MOS cameras into a single lightcurve. Figure 1 shows the 2 - 10 keV lightcurve of X41.4+60. The average 2 - 10 keV countrate in the PN + MOS is 3.18 s^{-1}.

2.1. Power Spectral Timing Analysis

We calculated a single FFT power spectrum using a lightcurve sampled at 1/2 s, yielding a 1 Hz Nyquist frequency. We used only the time interval for which both the PN and MOS were operating. This gave a continuous exposure of $\approx$ 27 ksec. Figure 2 shows the 2 - 10 keV power spectrum rebinned by a factor of 128 in frequency space (frequency resolution 4.7 mHz) for the PN + MOS (lower curve), the PN only (middle curve), and the MOS only (sum of MOS1 and MOS2, top curve). There is a prominent QPO peak centered near 54 mHz in all three power spectra. To assess the significance of the QPO we fit the power spectrum using a model composed of a constant plus a power law and a Lorentzian. This model provides a good fit, giving a minimum $\chi^2 = 185$ with 206 degrees of freedom (dof), and is shown in Figure 2 as the solid curve through the PN + MOS spectrum. If the Lorentzian (QPO) component is excluded from the model, the fit is unacceptable, with a minimum $\chi^2 = 255$. This gives a $\Delta\chi^2 = 70$ for the additional 3 parameters of the QPO component. The significance of the additional parameters can be estimated with the F-test, and gives a probability of $\approx 3 \times 10^{-14}$, which strongly indicates the need for the QPO component.

To make another estimate of the significance of the QPO we used the power law parameters from our best fit model to rescale the power spectrum so that the local mean power in the vicinity of the QPO was 2, the level expected for pure counting noise in the spectrum. The probability of obtaining by chance the highest power, $P_{max} = 3.28$, in the QPO profile is then just the probability of obtaining a power $P = P_{max} \times 128$ from the χ^2 distribution with $2 \times 128 = 256$ degrees of freedom (this because we averaged 128 independent powers in rebinning the spectrum). This gives a single trial probability of 4.5×10^{-10} for the highest power seen in the QPO profile. Multiplying by the number of powers searched, $N_{trials} = 212$, in the power spectrum then gives a significance of 9.5×10^{-8}, which is about a 6σ detection. Based on this and the F-test estimate above, we are very confident in the QPO detection.

When we construct lightcurves using the PN events at higher sampling frequencies and compute power spectra we clearly see the 13.63 Hz (73 ms) frame sampling rate, its harmonics, and aliases of some of the harmonics. The 54 mHz QPO cannot be due to an alias of this sampling frequency. The aliases of its first several harmonics are not at or

near the measured QPO frequency, and any aliased power from higher harmonics is greatly suppressed by the time binning. These features are also narrow, whereas the QPO is not. Similar arguments hold for the MOS analysis. When we analyse only photons with energies less than 2 keV the QPO is not detected, indeed, there is no indication of any significant variability. This is consistent with the conclusion that most of the soft X-ray flux is from the diffuse emission in the XMM beam, and also provides additional evidence that the QPO is not due to some instrumental signature.

Our best power spectral model includes a power law component, $A\nu^{-\alpha}$, with $\alpha = 1 \pm 0.12$, and an integrated variability (rms) of 13.5% from 0.1 mHz to 1 Hz. The QPO has a centroid frequency of 54.4 ± 0.9 mHz,a width $\Delta\nu_{fwhm} = 11.4 \pm 2$ mHz, and an amplitude (rms) of 8.4% in the 2 - 10 keV band. We searched for energy and time dependence of the QPO amplitude, but did not find any strong dependence. However, due to the relatively low signal to noise ratio, the data are not particularly sensitive to either of these effects.

2.2. RXTE Timing Analysis

Based on our XMM detection we decided to search archival RXTE observations for similar timing features. Indeed, $\sim$ 100 ksec of monitoring observations were carried out on M82 with RXTE from February to November of 1997 (Proposal ID 20203; see Gruber & Rephaeli 2002). These were typically 3 - 4 ksec pointings utilizing 3 of the 5 Proportional Counter Array (PCA) detectors. We extracted lightcurves with a 128 Hz sampling rate using only the top xenon layer and events in the 2 - 20 keV energy band. Here we only summarize results from several of the observations with indications of QPOs in the 50 - 100 mHz range. A complete analysis of the timing properties of all the observations will be presented in a sequel. Figure 3 shows power spectra from three observations with QPO detections. Each power spectrum is labelled with the corresponding observation ID. Model fits including a power law and a Lorentzian are also shown.

The two most significant QPOs are in the 20203-02-04-00 and 20203-02-02-00 observations. These QPOs have frequencies of 107 ± 3 mHz, and 51 ± 2 mHz, and F-test significances of 1.7×10^{-6} and 3.2×10^{-6}, respectively. To determine the QPO amplitudes we first computed background countrates using the RXTE/PCA background models. This gave 2 - 20 keV source counting rates of $\approx 8 - 9$ s^{-1}, and corresponding amplitudes (rms) of about 8 % for each QPO. The QPO frequencies, amplitudes and coherences inferred from the RXTE data are very similar to those derived from the XMM data. As we discuss below, the flux levels inferred for the RXTE observations with QPOs are consistent with the XMM flux level. The similar flux levels and QPO properties suggest that the source was in a similar state (see

Gruber & Rephaeli 2002). However, the RXTE monitoring also found the source at a flux level higher by a factor of 3 on 4 occasions. Interestingly, these observations did not reveal any evidence for QPOs, even though the counting rate was higher and therefore the QPO sensitivity was better. These observations provide direct evidence of a correlation between spectral states and timing properties, a common feature of accreting compact objects.

2.3. Energy Spectral Analysis

We obtained the spectrum of X41.4+60 by extracting a region with radius of 18", excising the resolved source to the north-east. This extraction region has extensive diffuse emission which is spatially resolved by Chandra (see for example, Kaaret et al. 2001). Fitting the Chandra spectrum of the bright point source one derives an effective column density of $0.5 - 0.9 \times 10^{21}$ cm^{-2} depending on the continuum model used. We then fit the XMM data in the 3 - 10 keV band from all 3 instruments. We find that a power law model is considerably worse than a disk blackbody (diskbb) or comptonized (compst) model (minimum $\chi^2 = 2907$ vs 2385 or 2246, with 2021 dof), with the column density fixed to the range allowed by the Chandra data. Further, no significant reduction in χ^2 is obtained for more complex continuum models (e.g. the addition of a power law to a diskbb model) often used to model Galactic BHCs. However, there are broad residuals in the spectrum no matter what continuum model is used. These residuals can be modelled by a variety of line shapes, including a relativistic broad line (the Laor model in XSPEC), the standard diskline model with extreme parameters ($q = -5.8$ with the diskbb continuum), or a gaussian. These fits indicate that much of the flux in the line comes from regions close to the black hole. The derived parameters for the line are, however, sensitive to the continuum model used. The most "curved" continuum, the compst model, has the lowest EW (230 eV) while the powerlaw model (which fits the continuum poorly) has an EW of 1300 eV. There is no evidence for a reflection component. Fitting a simple power law model in the 5 - 10 keV band (and not including any line emission) overpredicts the flux in the 3 - 5 keV band by a factor of ≈ 1.6 and does not account for the obvious line. The line is centered at 6.55 keV (1σ range of 6.48 - 6.60 keV) and has a gaussian width of 0.33 (0.26 - 0.43) keV. Figure 4 shows the total spectrum of M82 inside the 18" extraction radius.

The derived diskbb temperature, T_{BB}, is somewhat sensitive to the choice of column density, however, values less than 3 keV are strongly excluded. The 2 - 10 keV flux is 2.1×10^{-11} ergs cm^{-2} s^{-1}. The bolometric flux of the compst model is 3.3×10^{-11} ergs cm^{-2} s^{-1}, while that of the diskbb model is 3.5×10^{-11} ergs cm^{-2} s^{-1}. Using a distance of 3.5 Mpc this gives bolometric luminosities of $\approx 4 - 5 \times 10^{40}$ ergs s^{-1}. Assuming a similar spectrum,

the bolometric luminosity of the object during the 4 brightest RXTE observations is 3× larger or $\sim 1 \times 10^{41}$ergs s^{-1}.

3. Discussion and Summary

The discovery of QPOs from an extra-galactic compact object has many important implications. First, it establishes beyond doubt the compact nature of the source. A firm upper limit to the size of the hard X-ray emission region from the QPO timescale is, $r_{source} < c/\nu_{QPO} = 2.8 \times 10^6$ km, which is about 4 $R_\odot$. If the highest frequency QPO is associated with the Kepler frequency at the last stable circular orbit around a Schwarzschild black hole, then the mass must be $M_{bh} < 1.87 \times 10^4 M_\odot$. This establishes the ULX in M82 as a stellar-sized object and not an AGN. Based on QPO timescales found in the well studied Galactic black holes it also seems likely that the actual size of the emission region is substantially less than the above limit.

Several Galactic microquasars, for example, GRS 1915+105, GRO J1655-40 and XTE J1550-564, show low frequency QPOs with similar frequency and strength as the QPOs from X41.4+60 described here (see Morgan, Remillard & Greiner 1997; Remillard et al. 1999; and Cui et al. 1999). For example, GRS 1915+105 shows $\sim 10 - 100$ mHz QPOs at times when the source is in a "bright" state characterized by relatively modest broad band variability ($10 - 15\%$ rms, see Morgan, Remillard & Greiner 1997). To the extent that they can be compared, the timing properties of GRS 1915+105 in this state are similar to the properties of X41.4+60 reported here. The QPO frequencies, amplitudes and coherences are similar, as is the power law index and strength of the broad band variability. The energy spectrum of GRS 1915+105 in such a state is also qualitatively similar to the inferred spectrum of X41.4+60, being fit by a relatively hot disk-blackbody component, although the inferred inner disk temperature is higher for X41.4+60. GRO J1655-40 has also shown $80 - 100$ mHz QPOs when the spectrum has high inferred disk temperatures (see Remillard et al. 1999; Sobczak et al. 1999).

At first glance these comparisons would seem to suggest that X41.4+60 may be an analog of the Galactic microquasars, and thus that its mass is not extreme (se Greiner, Cuby & McCaughrean 2001). However, there is a substantial difficulty with this conclusion. Detection of strong, narrow QPOs provides compelling evidence for the presence of a geometrically thin accretion flow (i.e a disk, see van der Klis 1995; Di Matteo & Psaltis 1999), which effectively rules out any substantial beaming, either geometric or relativistic. For example, Madau (1988) has computed spectra from thick accretion disks which can have beaming factors approaching 25. The radiation field along the rotation axis is greatly enhanced by

the multiple scattering of photons off the walls of the inner, very hot and luminous, funnel-shaped region. It is found that the funnel dominates the emission from tori which are viewed at small angles from the symmetry axis. The presence of a narrow QPO effectively rules out such a scenario for X41.4+60, since multiple scatterings would degrade and broaden any QPO variability. We note that the $\approx$ 7 hr periodic dipping/eclipsing modulation seen in a ULX in the Circinus Galaxy (Bauer et al. 2001) also argues strongly against substantial beaming in this source. One is then left with the need to account for a luminosity $\approx 100\times$ that of GRS 1915+105 without the ability to invoke substantial beaming.

Galactic black hole binaries also show $\sim 0.8 - 3$ Hz QPO in the "very-high" state (van der Klis 1995; Cui et al. 1999; Morgan, Remillard & Greiner 1997). These "disk - corona" oscillations are associated with a non-thermal (power law) spectral component (see Swank 2001 for a review). These states show a characteristic flat-topped, broad band noise which breaks to a steeper power law at about the QPO frequency (see Morgan, Remillard & Greiner 1997 for examples from GRS 1915+105). Could the QPOs in X41.4+60 be the analog of these $\sim$ 1 Hz QPOs? Assuming that frequencies scale roughly as $1/M_{bh}$ suggests a mass of order $100 - 300 M_{\odot}$ to obtain a 54 - 100 mHz QPO. However, the broad band variability below the QPO in X41.4+60 is really not flat-topped, and the lack of a non-thermal (power law) component in X41.4+60 also distinguishes this object from Galactic BHCs in this state.

Accreting X-ray pulsars (neutron stars) can also show QPOs with frequencies in the $\sim$ 50 mHz range (see Takeshima 1992; Shinoda et al. 1990). These objects can also show broad band noise similar to the low state noise seen in Galactic BHCs and the high state noise in atoll sources (van der Klis 1995). Perhaps surprisingly, accreting pulsars can also be extremely luminous. For example, the famous "bursting pulsar" GRO J1744-28 has produced short lived (10 - 20 second) Type II bursts with peak luminosities of $\approx$ 100 times the Eddington limit for a neutron star (see Jahoda et al. 1997). Although we do not detect any strictly periodic emission from X41.4+60, the fact that neutron star systems produce QPOs with frequencies similar to the 54 mHz QPO in X41.4+60, and can also be super-Eddington, suggests that in some scenarios extreme masses may not be necessary to explain high isotropic luminosities.

We are left with something of a conundrum; the presence of strong, narrow QPOs argues strongly that most of the flux in the 3 - 9 keV band originates from a disk, and thus the emission is not strongly relativistically or geometrically beamed. However no present disk models (Gierlinski et al 2002) can produce a color temperature as high as seen in X41.4+60. The inferred inner disk radius using the diskbb model is $\approx$ 35 km (assuming $T_{BB} = 3.1 keV$, a distance of 3.5 Mpc, an inclination angle of 45°, and no spectral hardening corrections). A Schwarzschild black hole of $4 M_{\odot}$ would have a last stable orbit this size. This

further highlights the luminosity problem, and suggests that the diskbb model is probably unphysical, indeed, a comptonization model seems more plausible. Since we now know that the radiation is not beamed it is also extremely difficult to explain the observed very high long term bolometric luminosity with an object of $< 300\ M_{\odot}$ despite the apparent difficulties with such a scenario. The QPO frequency and the broad Fe K line are reminiscent of that seen in the Galactic microquasars in the VHS, but the continuum is rather different. We are thus left with the intriguing possibility that these objects show behavior not seen in any other black holes candidates, either in the Milkyway or as AGN.

Our results indicate that a combination of sensitive X-ray timing and spectroscopy can provide new insights into the nature of ULXs. Future missions with even larger collecting area, good spatial and spectral resolution and timing capabilities (such as Constellation-X and XEUS), should be able to open up a new window on the properties of black holes in the local universe.

We thank Keith Arnaud, Craig Markwardt and Jean Swank for many helpful discussions and comments on the manuscript.

REFERENCES

Bauer, F. E. et al. 2001, AJ, 122, 182.

Colbert, E. J. M. & Mushotzky, R. F. 1999, ApJ, 519, 89.

Cui, W., Zhang, S. N., Chen, W. & Morgan, E. H. 1999, ApJ, 512, L43.

Di Matteo, T. & Psaltis, D. 1999, ApJ, 526, L101.

Fabbiano, G. 1988, ApJ, 330, 672.

Fabbiano, G. & Trinchieri, G. 1987, ApJ, 315, 46.

Greiner, J., Cuby, J. G. & McCaughrean, M. J. 2001, Nature, 414, 522.

Grimm, H.-J., Gilfanov, M. & Sunyaev, R. 2002, MNRAS, in press, (astro-ph/0205371).

Gruber, D. & Rephaeli, Y. 2002, A&A, 389, 752.

Jahoda, K. et al. 1997, in The Active X-ray Sky: Results from BeppoSAX and RXTE. Edited by L. Scarsi, H. Bradt, P. Giommi, and F. Fiore. Publisher: Amsterdam: Elsevier, 1998, Reprinted from: Nuclear Physics B, (Proc. Suppl.), vol. 69/1-3.

Kaaret, P. et al. 2001, MNRAS, 321, L29.

King, A. R., Davies, M. B., Ward, M. J., Fabbiano, G. & Elvis, M. 2001, ApJ, 552, L109.

Kubota, A., Done, C. & Makishima, K. 2002, MNRAS, 337, L11.

Madau, P. 1988, ApJ, 327, 116.

Makishima, K. et al. 2000, ApJ, 535, 632.

Matsumoto, H. et al. 2001, ApJ, 547, L25.

Miller, J. M., Fabbiano, G., Miller, M. C., & Fabian, A. C. 2002, ApJ, submitted (astro-ph/0211178).

Morgan, E. H., Remillard, R. A. & Greiner, J. 1997, ApJ, 482, 993.

Muno, M. P., Morgan, E. H. & Remillard, R. A. 1999, ApJ, 527, 321.

Portegies Zwart, S. F. & McMillan, S. L. W. 2002, ApJ, 576, 899.

Ptak, A. & Griffiths, R. 1999, ApJ, 517, L85.

Remillard, R, A., Muno, M. P., McClintock, J. E. & Orosz, J. A. 2002, in Procs. of the 4th Microquasar Workshop, 2002, eds. Durouchoux, Fuchs, & Rodriguez, (Center for Physics: Kolkata), (astro-ph/0208402).

Remillard, R. A., Morgan, E. H., McClintock, J. E., Bailyn, C. D. & Orosz, J. A. 1999, ApJ, 522, 397.

Schlegel, E. M. 1994, ApJ, 424, L99.

Shinoda, K. et al. 1990, PASJ, 42, L27.

Sobczak, G. J., McClintock, J. E., Remillard, R. A., Bailyn, C. D. & Orosz, J. A. 1999, ApJ, 520, 776.

Swank, J. H. 2001, Astroph. & Space Sci., 276 (suppl.), 201.

Takeshima, T. 1992, Ph.D. thesis, University of Tokyo.

van der Klis, M. 1995, in X-ray Binaries, ed. Lewin, van Paradijs & van den Heuvel (Cambridge University Press: Cambridge), pg. 252.

Zezas, A. & Fabbiano, G. 2002, ApJ, 577, 726.

4. Figure Captions

Fig. 1.— EPIC PN + MOS lightcurve of the ULX near the central region of M82. The time bins are 64 seconds. A characteristic error bar is also shown.

Fig. 2.— Power spectrum of the EPIC > 2 keV data from X41.4+60. The Nyquist frequency is 1 Hz. The frequency resolution is 4.7 mHz. The Poisson level has not been subtracted. Shown are the power spectra from the combined PN + MOS data (lower), the PN only (middle), and MOS only (top). The best fitting power law + Lorentzian model is shown as the thick solid curve (lower).

Fig. 3.— Power spectra from three RXTE observations of M82 which show low frequency QPOs. Each spectrum is labelled with the corresponding OBSID. The best fit models are also shown. For each spectrum a typical error bar near the peak of the QPO feature is shown. The error bar for the middle curve (20203-02-04-00) has the same size as that shown for the bottom curve (20203-02-02-00).

Fig. 4.— The countrate spectrum in the PN inside the 18" extraction radius. The soft excess is from the diffuse thermal emission, and was constrained based on Chandra observations which resolved the diffuse component. The emission above 2 keV is dominated by the point source.

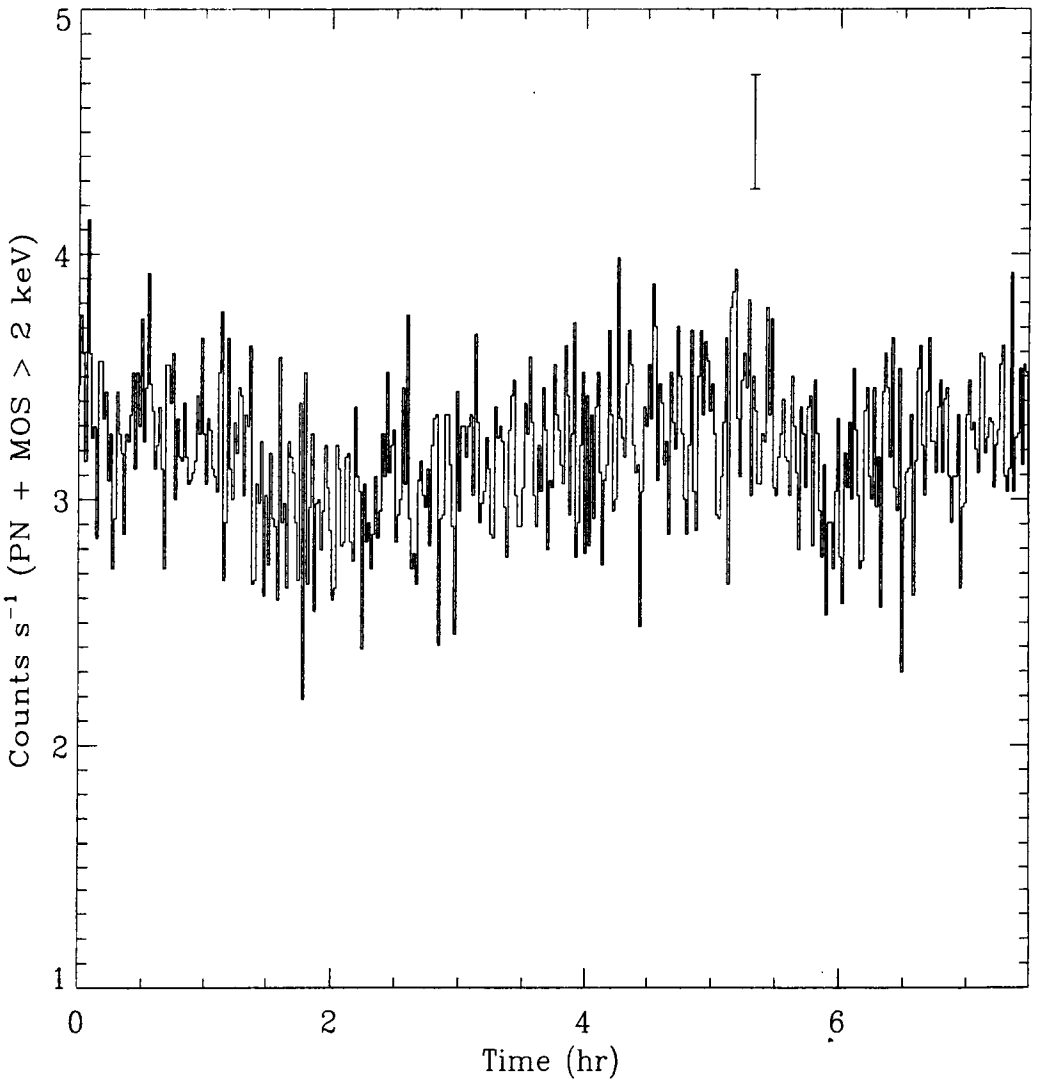

Figure 1: EPIC PN + MOS lightcurve of the ULX near the central region of M82. The time bins are 64 seconds. A characteristic error bar is also shown.

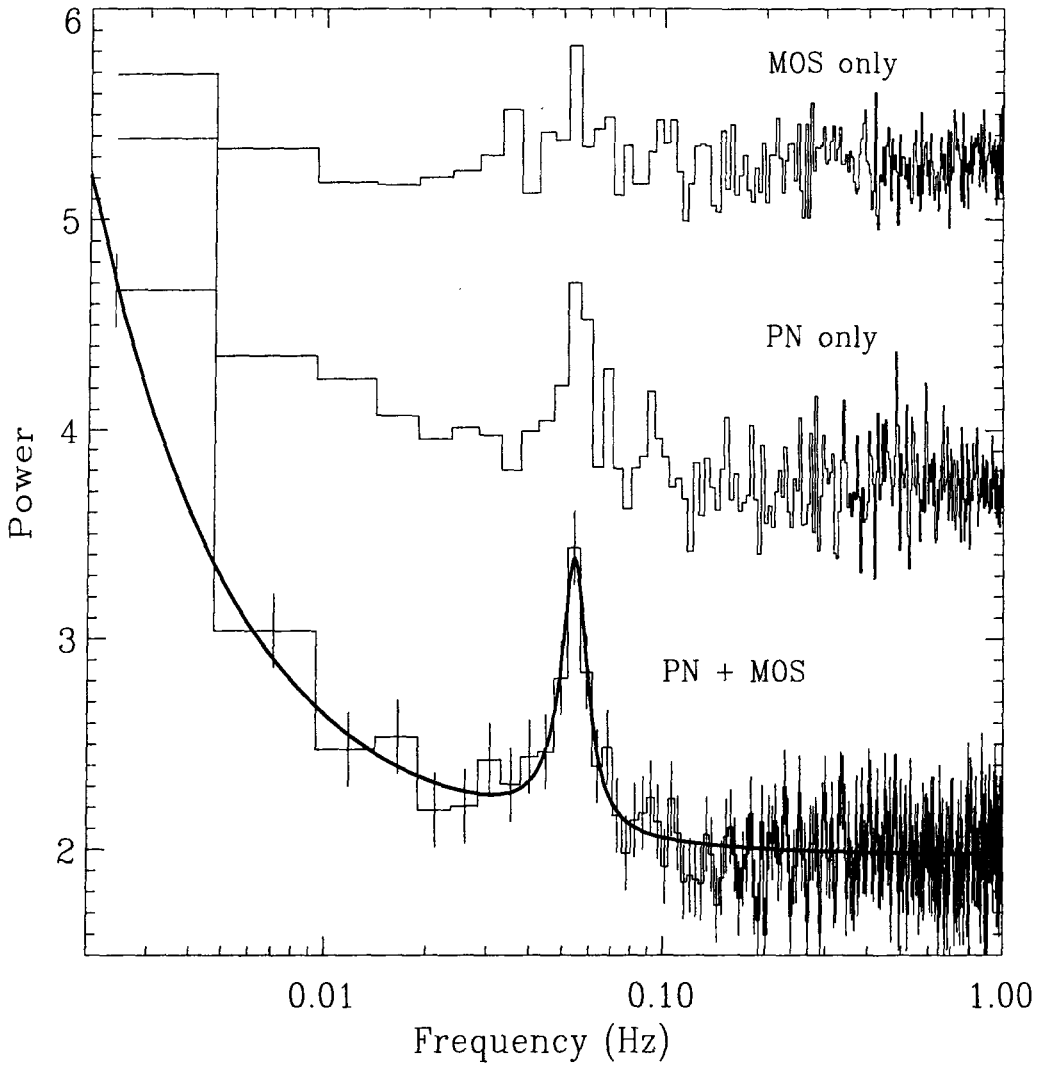

Figure 2: Power spectrum of the EPIC > 2 keV data from X41.4+60. The Nyquist frequency is 1 Hz. The frequency resolution is 4.7 mHz. The Poisson level has not been subtracted. Shown are the power spectra from the combined PN + MOS data (lower), the PN only (middle), and MOS only (top). The best fitting power law + Lorentzian model is shown as the thick solid curve (lower).

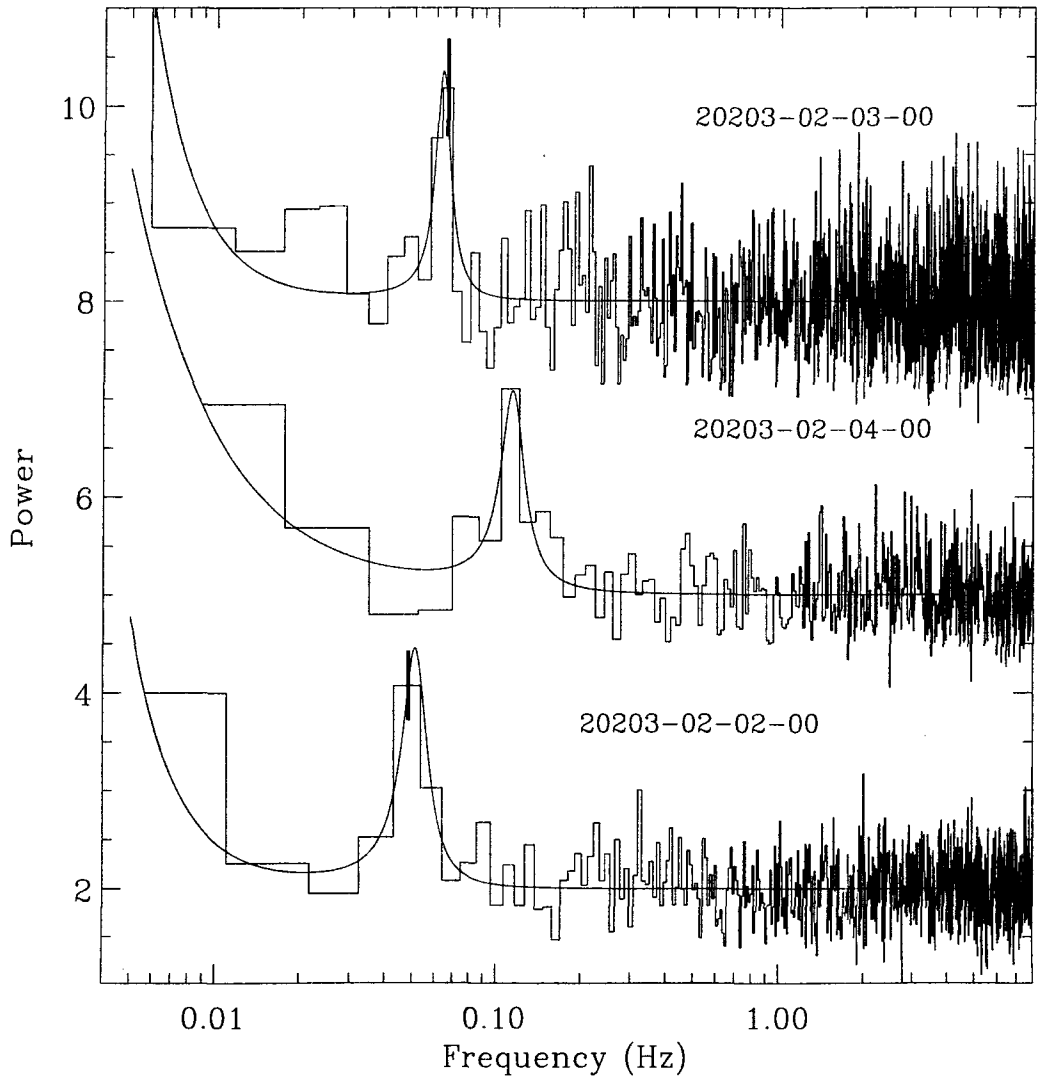

Figure 3: Power spectra from three RXTE observations of M82 which show low frequency QPOs. Each spectrum is labelled with the corresponding OBSID. The best fit models are also shown. For each spectrum a typical error bar near the peak of the QPO feature is shown. The error bar for the middle curve (20203-02-04-00) has the same size as that shown for the bottom curve (20203-02-02-00).

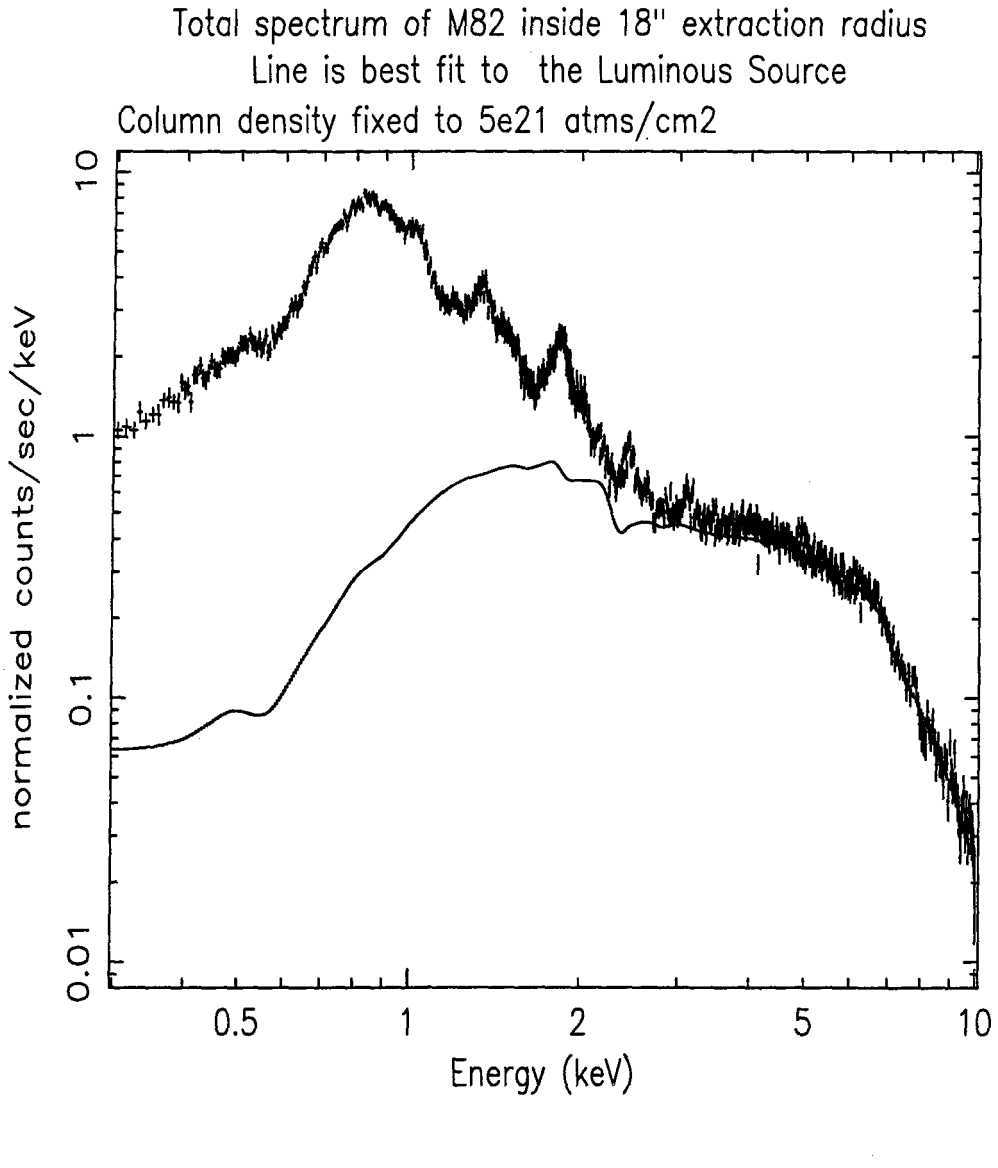

Figure 4: The countrate spectrum in the PN inside the 18" extraction radius. The soft excess is from the diffuse thermal emission, and was constrained based on Chandra observations which resolved the diffuse component. The emission above 2 keV is dominated by the point source.